

Supporting Information

Wrinkles in 2D TMD Heterostructures: Unlocking Enhanced Hydrogen Evolution Reaction Catalysis

Kai Ren¹, Feifan Wang², Tianyang Liu², Huasong Qin^{3,*} and Yu Jing^{2,*}

¹School of Mechanical and Electronic Engineering, Nanjing Forestry University, Nanjing, Jiangsu 210037, China

²Jiangsu Co-Innovation Centre of Efficient Processing and Utilization of Forest Resources, College of Chemical Engineering, Nanjing Forestry University, Nanjing 210037, China

³Laboratory for Multiscale Mechanics and Medical Science SV LAB, School of Aerospace Xi'an Jiaotong University, Xi'an 710049, China

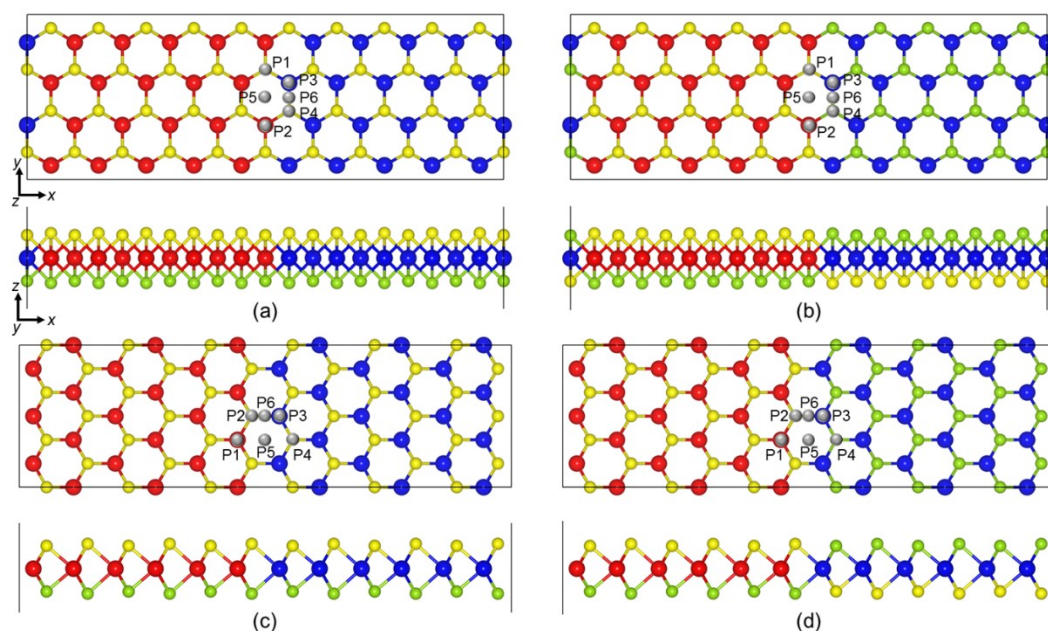


Figure S1. Atomic structure of the MoSSe/WSSe lateral heterostructure with (a) Armchair-1, (b) Armchair-2, (c) Zigzag-1 and (d) Zigzag-2 interface configuration, the gray ball at the interface indicates the possible adsorption sites for H. Red, blue, yellow and the cyan spheres represent the Mo, W, S and Se atoms, respectively.

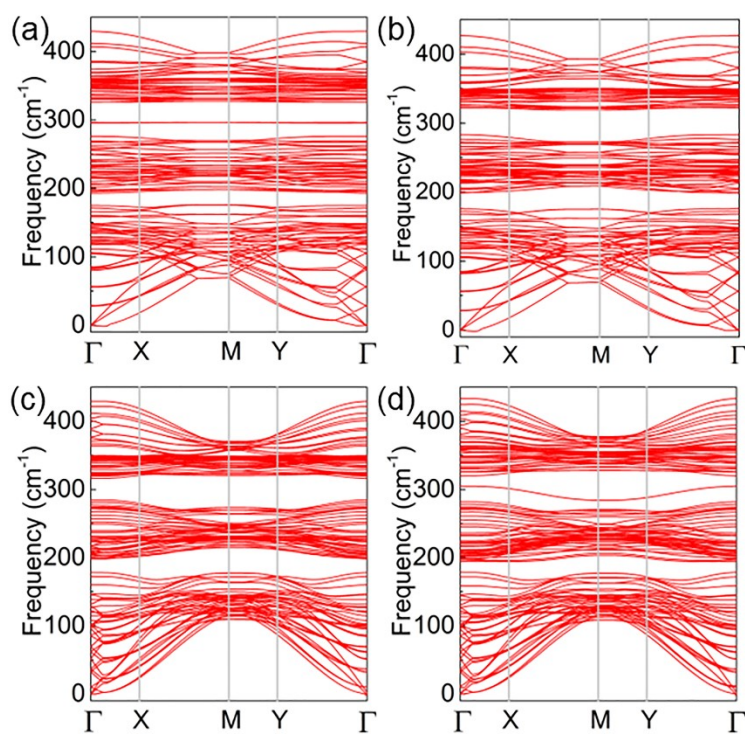


Figure S2. Phonon dispersions of the (a) Armchair-1, (b) Armchair-2, (c) Zigzag-1 and (d) Zigzag-2 MoSSe/WSSe lateral heterostructures.

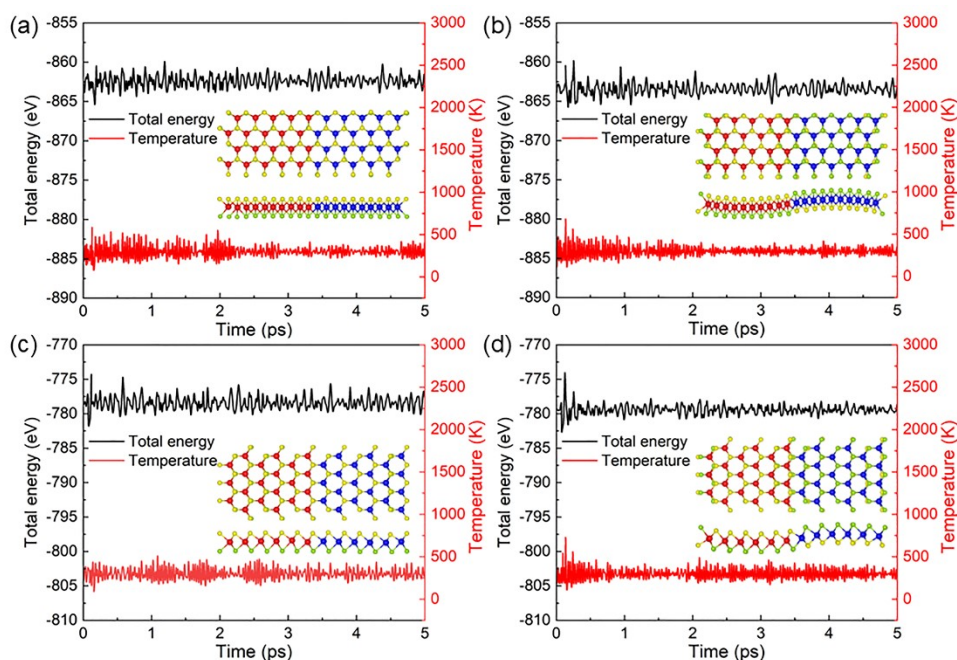


Figure S3. The energy variation of the (a) Armchair-1, (b) Armchair-2, (c) Zigzag-1 and (d) Zigzag-2 MoSSe/WSSe lateral heterostructures in AIMD calculations, the insets demonstrate the snapshots of the studied system.

The geometric expression of Janus heterostructure can be described by using Euler–Bournelli beam model:¹

$$\frac{d^2}{dx^2} \left(D \frac{d^2 w}{dx^2} \right) = 0, \quad (\text{S1})$$

where w represents the deflection, D is the effective bending stiffness. The boundary conditions are defined by the fractional coordinates of the atoms along the z -axis, with Δz representing the difference between the z -coordinates of all atoms and the initial atom. The resulting deflection can thus be described by Δz as:

$$w(x) = \frac{ML^2}{24D} \left[-\left(\frac{2x-L}{L} \right)^3 + 3\left(\frac{2x-L}{L} \right)^2 - 2\left(\frac{2x-L}{L} \right) \right], \quad (\text{S2})$$

where the L is the length of the heterostructure. One can see that the fitted function of the trajectory is consistent, suggesting the wrinkled MoSSe/WSSe interface can be tuned by Euler–Bournelli beam theory.

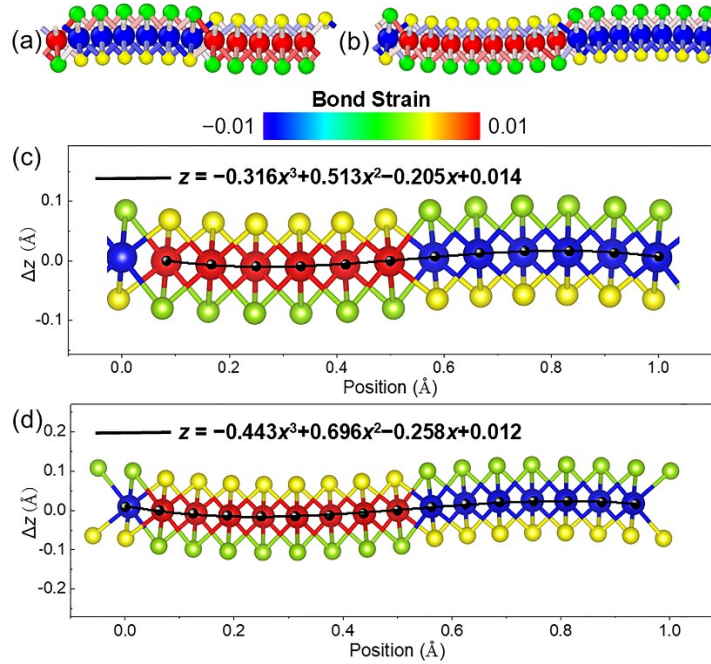


Figure S4. (a, b) The bond strain and the (c, d) the fitted Euler–Bournelli beam curve of the Armchair-2 MoSSe/WSSe lateral heterostructure by (a, c) 12 and (b, d) 16 unit-cells.

Table. S1 The binding energy (E_b , eV) of H on MoSSe/WSSe heterostructures at different adsorption sites as illustrated in Figure. S1. The Janus site denotes the opposite side of the adsorption position.

	Armchair-1	Armchair-2	Zigzag-1	Zigzag-2
P1	-0.35	0.19	2.15	2.71
P2	-0.30	0.03	2.23	2.78
P3	-0.37	0.02	3.12	3.68
P4	-0.28	0.06	2.41	2.96
P5	-0.47	0.25	2.12	1.73
P6	-0.30	-0.10	2.25	2.81
Janus P1	-0.22	-0.33	2.60	3.15
Janus P2	-0.12	0.03	2.78	3.33
Janus P3	-0.21	-0.14	3.01	3.56
Janus P4	-0.20	0.27	2.43	2.98
Janus P5	-0.22	-0.06	2.52	3.07
Janus P6	-0.20	0.24	2.64	3.19

The HER performance of these MoSSe/WSSe lateral heterostructures is examined by calculating the Gibbs free energy (ΔG_{H^*}) according to:²

$$\Delta G_{H^*} = \Delta E + \Delta E_{zpe} + T\Delta S, \quad (S3)$$

where ΔE denotes the total energy of the H adsorbed MoSSe/WSSe heterostructure, ΔE_{zpe} represents the change in zero-point energy, T denotes the temperature and is treated as 298.15 K in this work. The difference in entropy after the adsorption of H is defined by ΔS . “*” is marked as the active site of the HER within the heterostructure. Furthermore, the HER process of the MoSSe/WSSe lateral heterostructure is studied by looking into the two elementary steps:³



The projection band center of the MoSSe/WSSe heterostructure is calculated by:

$$\varepsilon = \frac{\int_{-\infty}^{\infty} x\rho(x)dx}{\int_{-\infty}^{\infty} \rho(x)dx} \quad (S6)$$

The charge density difference ($\Delta\rho$) of the H-absorbed MoSSe/WSSe lateral heterostructure is calculated by:

$$\Delta\rho = \rho_{\text{H-hetero}} - \rho_{\text{H}} - \rho_{\text{hetero}} \quad (S7)$$

where the $\rho_{\text{H-hetero}}$, ρ_{H} , and ρ_{hetero} represent the charge density of the H absorbed system, individual H, and the pure MoSSe/WSSe heterostructure, respectively.

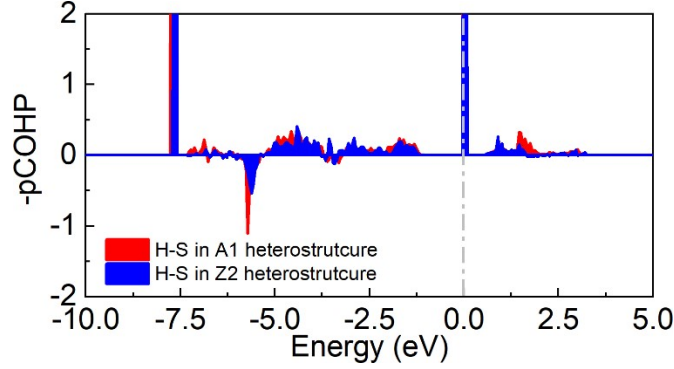


Figure S5. The orbital contribution of pCOHP between intermediates (H^*) on the Armchair-1 and Zigzag-2 MoSSe/WSSe heterostructures.

The atomic virial pressure of atoms in MoSSe/WSSe heterostructure is calculated as:⁴

$$\sigma_i = \frac{1}{\Omega_i} \left[m_i v_i \otimes v_i + \frac{1}{2} \sum_{j \neq i} F_{ij} \otimes r_{ij} \right] \quad (S8)$$

where the volume, mass, and velocity vectors for the atom i are represented as Ω_i , m_i , and v_i , respectively. The F_{ij} represents the force of atom i applied on atom j . The r_{ij} shows the distance between atom i and j . Furthermore, the symmetric stress tensor (σ_i) can be composed as σ_{xx} , σ_{yy} , σ_{zz} , σ_{xz} , σ_{xy} , and σ_{yz} , where σ_{xz} , σ_{yz} , and σ_{zz} can be ignored in the 2D MoSSe/WSSe heterostructure system.⁵

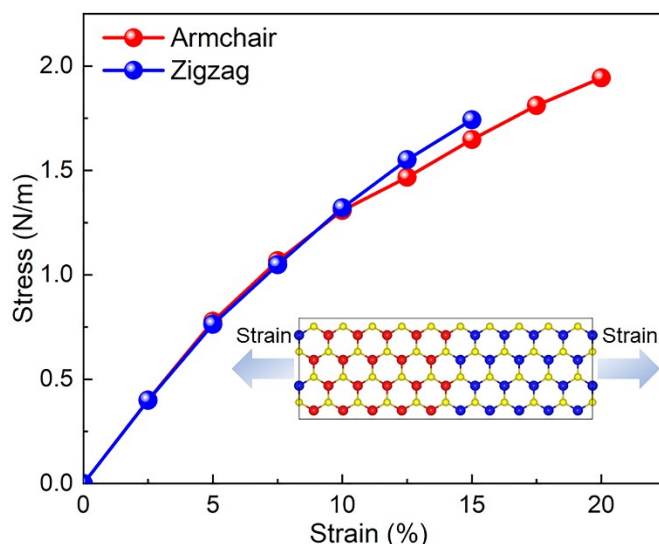


Figure S6. The calculated stress–strain curves of the MoSSe/WSSe lateral heterostructure with Armchair-2 (red line) and Zigzag-2 (navy line) interface.

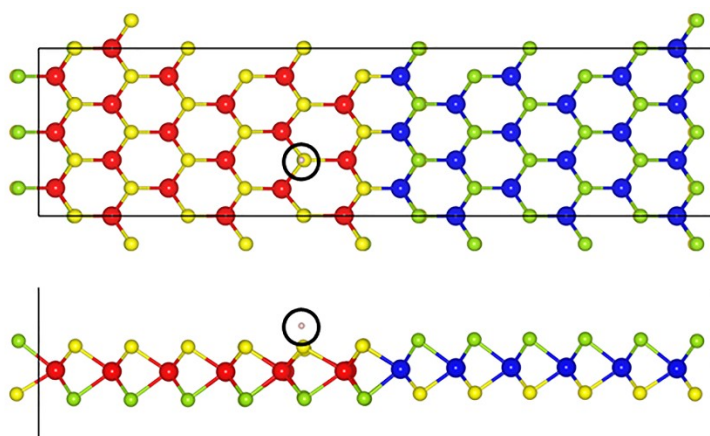


Figure S7. The obtained H adsorbed Zigzag-2 MoSSe/WSSe heterostructure under the strain of 17%.

References

1. Gere, J. M.; Timoshenko, S. P., *Mechanics of Materials*. Brooks/Cole **2004**, 599.
2. Ren, K.; Shu, H.; Wang, K.; Qin, H., Two-Dimensional MX_2Y_4 Systems: Ultrahigh Carrier Transport and Excellent Hydrogen Evolution Reaction Performances. *Phys. Chem. Chem. Phys.*, **2023**, *25*, 4519–4527.
3. Ren, K.; Shu, H.; Huo, W.; Cui, Z.; Xu, Y., Tuning Electronic, Magnetic and Catalytic Behaviors of Biphenylene Network by Atomic Doping.

Nanotechnology., **2022**, *33*, 345701.

4. Zhou, M., A New Look at the Atomic Level Virial Stress: On Continuum-Molecular System Equivalence. *P. Roy. Soc. a-Math. Phys.*, **2003**, *459*, 2347–2392.
5. Chung, J. Y.; Sorkin, V.; Pei, Q. X.; Chiu, C. H.; Zhang, Y. W., Mechanical Properties and Failure Behaviour of Graphene/Silicene/Graphene Heterostructures. *J. Phys. D-Appl. Phys.*, **2017**, *50*, 345302.